

# OXIDATION OF HIGH-TEMPERATURE ALLOY WIRES IN DRY OXYGEN AND WATER VAPOR

Elizabeth J. Opila, Jonathan A. Lorincz<sup>&</sup>,  
Jeffrey J. DeMange\*,

NASA Glenn Research Center, Cleveland, OH 44135

<sup>&</sup>Ohio University, Athens, OH

\*University of Toledo, Toledo, OH

High-temperature alloy wires are proposed for use in seal applications in future space vehicles. The alloys offer the potential for improved wear resistance of the seals. However, the wires must withstand high-temperature environments which contain both oxygen and water vapor. In this study, alloy wires are evaluated for oxidation resistance in dry oxygen and oxygen/water vapor environments.

Five compositions of alloy wires were studied as shown in Table 1. All wires were nominally 250 micrometers in diameter, except the PM2000 which had a nominal diameter of 150 micrometers. Coils of wire were formed to achieve a total surface area of about 3 to 5 cm<sup>2</sup>. The coiled wires were oxidized in flowing oxygen at 1204°C for 70h. Several compositions were also tested in 50% water vapor/50% oxygen. Oxidation kinetics were continuously monitored by thermogravimetry (TGA). Post-test analysis included X-Ray Diffraction (XRD), Scanning Electron Microscopy (SEM) and Energy Dispersive Spectroscopy (EDS) for phase identification and morphology.

The weight change results for dry oxygen tests are shown in Figure 1. As expected, the alumina forming alloys, Kanthal A1 and PM2000 performed the best. Weight change results for water vapor tests for these two compositions plus the baseline material Haynes 188 are shown in Figure 2. Again, the alumina-forming compositions outperformed the Haynes 188.

The oxidation resistance of these alloys is predictable since alumina-forming alloys are expected to outperform chromia-forming alloys at this temperature. However, the water vapor results as well as features of the oxidation kinetics due to the small diameter of the wires provide interesting insights into oxidation behavior of these materials. Several of these results will be highlighted.

First, the Haynes 188 wires were found to completely oxidize under test in both dry oxygen and water vapor after 20 to 30 hours exposure. In dry oxygen the weight gain reached a plateau at 19 mg/cm<sup>2</sup> as complete oxidation occurred. Microstructural analysis shows compositional layering effects in the oxide as a result of sequential depletion of the chromium and tungsten components. In water vapor, however, a regime of linear weight loss began after about 20 hours as volatile hydroxide formation, e.g. WO<sub>2</sub>(OH)<sub>2</sub>(g) and Ni(OH)<sub>2</sub>(g), continued even after the wire was completely oxidized. Microstructural and compositional analysis of the wire after water vapor exposure shows the presence of porous layers as well as the complete loss of tungsten from the remaining oxide.

The Kanthal A1 wires showed excellent oxidation behavior in both dry oxygen and water vapor as determined by weight change kinetics. However, microstructural evaluation showed complete loss of adherence of the oxide scale for both test conditions, leaving detached sheaths of oxide. Bare metal wires with no trace of oxide were observed for some cross-sections of the Kanthal A1 exposed in water vapor.

The PM2000 wires showed excellent oxidation behavior in dry oxygen as determined by weight change kinetics. The discontinuity in weight change at 40 to 50h is

tentatively attributed to a change in oxide growth from alumina to chromia. EDS analysis indicated the aluminum content of the wires was completely depleted after the 70h exposure in dry oxygen. Microstructural analysis revealed adherent scales, an inner chromia-rich oxide layer, and outer alumina layers. Void formation within the metal wire interior was also observed. In the water vapor exposure, breakaway oxidation occurred just as the 70h test ended. EDS analysis indicated the aluminum content of the wires was also completely depleted after the water vapor exposures. Microstructural analysis revealed some cross-sections of the wire showed protective oxides, while others showed initial stages of breakaway oxidation with chromia and iron rich surface oxide formation. Still other areas of the same wire showed complete oxidation of the entire cross-section.

In conclusion, the alumina-forming wires outperform the baseline Haynes 188 composition for oxidation resistance at proposed seal conditions. Additionally, TGA of small diameter wires offers unique opportunities for studying oxide volatility, oxide adherence, and breakaway oxidation.

Table 1. Composition of alloy wires used in this study.

Alloy	Composition, wt%
Haynes 188	Co base, 22 Cr, 22 Ni, 14 W, Fe < 3, Mn < 1.25, 0.5 Si, 0.12 La, trace: C, B
Haynes 230	Ni base, 22 Cr, 14 W, Co < 5, Fe < 3, 2 Mo, 0.5 Mn, 0.4 Si, 0.3 Al, trace: C, La, B
Haynes 214	Ni base, 16 Cr, 4.5 Al, 3 Fe, 0.2 Si, trace: Mn, Zr, C, B, Y
Kanthal A1	Fe base, 22 Cr, 5.8 Al
PM 2000	Fe base, 20 Cr, 5.5 Al, 0.5 Ti, 0.5 Y <sub>2</sub> O <sub>3</sub>

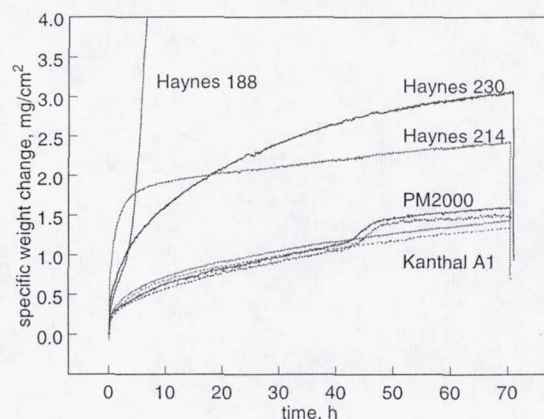


Figure 1. Specific weight change for coiled wires exposed at 1204°C, in dry O<sub>2</sub> flowing at 0.4 cm/s.

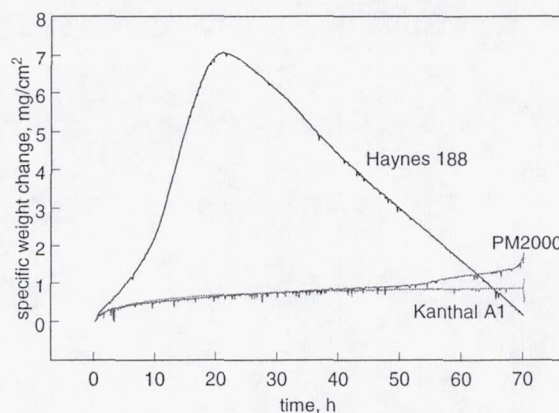


Figure 2. Specific weight change for coiled wires exposed at 1204°C, in 50% H<sub>2</sub>O/50% O<sub>2</sub> flowing at 4.4 cm/s.

## Acknowledgments:

The authors would like to acknowledge the help of Jim Smialek, Pat Dunlap, and Bruce Steinetz all of NASA Glenn Research Center. This work was funded by the Next Generation Launch Technology Program.

# OXIDATION OF HIGH-TEMPERATURE ALLOY WIRES IN DRY OXYGEN AND WATER VAPOR

Elizabeth J. Opila, Jonathan A. Lorincz<sup>&</sup>, and Jeffrey J. DeMange\*

NASA Glenn Research Center, Cleveland, OH 44135

<sup>&</sup>Ohio University, Athens, OH

\*University of Toledo, Toledo, OH

Small diameter wires (150 to 250  $\mu\text{m}$ ) of the high-temperature alloys Haynes 188, Haynes 230, Haynes 214, Kanthal A1 and PM2000 were oxidized at 1204°C in dry oxygen or 50% H<sub>2</sub>O/50% O<sub>2</sub> for 70 hours. The oxidation kinetics were monitored using a thermogravimetric technique. Oxide phase composition and morphology of the oxidized wires were determined by x-ray diffraction, field emission scanning electron microscopy, and energy dispersive spectroscopy. The alumina-forming alloys, Kanthal A1 and PM2000, out-performed the chromia-forming alloys under these test conditions. PM2000 was recommended as the most promising candidate for advanced hybrid seal applications for space reentry control surface seals or hypersonic propulsion system seals. This study also demonstrated that thermogravimetric analysis of small diameter wires is a powerful technique for the study of oxide volatility, oxide adherence, and breakaway oxidation.

## INTRODUCTION

High-temperature alloys are proposed for use in hybrid seal applications for future space vehicles (1). A hybrid seal is composed of a ceramic fiber or fabric core with an outer layer of wrapped or braided small diameter wire (40 to 125  $\mu\text{m}$ ). The wires offer significantly improved wear resistance when compared to ceramic fabrics (2). However, the wires must withstand environments which may contain oxygen and/or water vapor with operation temperatures up to 1400°C. These hybrid seals could be used in two types of space vehicle applications: 1) control surfaces and 2) propulsion systems. Advanced control surface seals are used to minimize the flow of high temperature gases through the gaps surrounding actuated structures such as body flaps and elevons. Accordingly, these seals help protect actuators (which control elevons and body flaps of space vehicles) and other temperature sensitive structures from the intense heat experienced in the reentry environment. Control surface seals are expected to operate in reduced pressure hot air or plasma with reusability requirements of 10 to 100 cycles of 30 minutes each. Hypersonic propulsion system seals are also designed to help shield actuated structures (e.g. actuators for moveable inlets) from heat damage. These seals are expected to operate in a propulsion environment containing high pressure water vapor and/or hydrogen. Reusability requirements are for 1000 cycles of 250 sec/cycle (70 hours total hot time) (3). Current state-of-the-art hybrid seals are composed of alumina or aluminosilicate fiber or batting core, wrapped with Haynes 188 or Haynes 230 wires. These seals are effective

This is a preprint or reprint of a paper intended for presentation at a conference. Because changes may be made before formal publication, this is made available with the understanding that it will not be cited or reproduced without the permission of the author.

to a maximum temperature of about 800°C based on both yield strength and oxidation limitations.

High-temperature alloy wire oxidation has been studied in the past for applications such as electric resistance alloys (4,5), and high temperature mesh or laminated metallic structures (6,7). In addition, small diameter wire geometry effects on growth stresses, oxidation kinetics, and spallation have been demonstrated (8-12). Oxidation of high-temperature alloys in water vapor has been a topic of great interest in recent years. In particular, the effects of water vapor on the oxidation of FeCrAl alloys included in the present study have been examined (13,14). It is proposed that water vapor causes more rapid oxidation in the earliest stages when mixed transient oxides are formed. At longer times, the oxidation rate is unaffected by water vapor. The overall effect of water vapor on the oxidation of FeCrAl alloys is slightly shorter times until formation of non-protective oxides.

The objectives of this paper are two-fold. First, the oxidation characteristics of high-temperature alloy wires are evaluated for advanced hybrid seal applications with higher temperature capability than current state-of-the-art. Second, opportunities for studying oxidation mechanisms that are enabled by the use of small diameter wires are presented.

## EXPERIMENTAL PROCEDURE

Five compositions of alloy wires were studied as shown in Table I. Haynes 188 and Haynes 230 are chromia-forming alloys. Haynes 214 is a marginal alumina-forming alloy while Kanthal A1 and PM2000 form alumina scales during oxidation.

Table I. Composition of alloy wires used in this study.

Alloy	Composition, wt%
Haynes 188	Co base, 22 Cr, 22 Ni, 14 W, Fe< 3, Mn <1.25, 0.5 Si, 0.12 La, trace: C, B
Haynes 230	Ni base, 22 Cr, 14 W, Co<5, Fe<3, 2 Mo, 0.5 Mn, 0.4 Si, 0.3 Al, trace: C, La, B
Haynes 214	Ni base, 16 Cr, 4.5 Al, 3 Fe, 0.2 Si, trace: Mn, Zr, C, B, Y
Kanthal A1	Fe base, 22 Cr, 5.8 Al, Si<0.7, Mn<0.4
PM 2000	Fe base, 20 Cr, 5.5 Al, 0.5 Ti, 0.5 Y <sub>2</sub> O <sub>3</sub>

The nominal diameter of all the wires, except PM2000, was 250µm. The diameter of the PM2000 wire was 150µm. The wires were oxidized in the condition as-received from the manufacturer. Sixty centimeter lengths of wire were coiled as shown in Figure 1. Due to the smaller wire diameter, the PM2000 wires were coiled in different configurations as will be seen in the results. The surface area of each coil varied between 3 and 5 cm<sup>2</sup>. The coiled wire was suspended from a sapphire hanger within a fused quartz furnace tube. The coils were oxidized in flowing oxygen (100 ccm, 0.4 cm/sec) at 1204°C ± 10°C for 70h. Haynes 188, Kanthal A1, and PM2000 coils were also oxidized in flowing 50% H<sub>2</sub>O/50% O<sub>2</sub> (1l/m, 4.4 cm/sec) at 1204°C for 70h. Oxidation kinetics were monitored by thermogravimetry (TGA). Post-test analyses included X-Ray Diffraction (XRD), Field Emission Scanning Electron Microscopy (FE-SEM), and Energy Dispersive Spectroscopy (EDS) for phase identification and morphology.

## RESULTS

### Dry oxygen

The weight change results for the five alloy compositions after exposure in dry oxygen at 1204°C for 70h are shown in Figure 2. The Haynes 188 wire showed protective oxide growth for about 3 hours before rapid weight gain occurred. The metal was totally consumed and converted to oxide after about 23 h of exposure based on the plateau in measured weight change. The Haynes 230 showed parabolic oxidation for the duration of the 70h test. Haynes 214 oxidized at an initial fast rate, then slowed down to a rate similar to those of the alumina-forming alloys Kanthal A1 and PM2000. As shown in Figure 2, the weight change results for Kanthal A1 and PM2000 were low and very repeatable. Repeat weight change measurements were obtained for only these two alloys. A brief increase in weight gain rate was observed for PM2000 at about 45 hours. One possible explanation for this behavior is that the aluminum content of the alloy was exhausted at 45 hours and chromia formation began. Note that a large weight loss occurred on cool-down for the Haynes 230, Haynes 214, and Kanthal A1. This weight change is attributed to oxide spallation and is much larger than any weight change that can be attributed to changes in sample buoyancy on cool-down. Very slight spallation occurred for one of the PM2000 wires on cool-down, but not for the other wire of the same composition.

Macrographs of the wires after oxidation are shown in Figure 3. The Haynes 188 wire retained its coil shape despite being completely oxidized; however, it was very brittle and damaged easily with handling. Evidence of spalling to bare metal was observed for the Haynes 214, Haynes 230, and Kanthal A1 wires. No evidence of bare metal spalling was observed for the PM2000.

X-ray diffraction (XRD) results of the oxidation products are summarized in Table 2. It should be pointed out that the XRD results were from powder samples obtained by crushing the wires, retained oxide, and spalled oxide. The resulting XRD sample is therefore concentrated in those oxides that spall off or can be easily ground off the oxidized wires. Oxidation products are listed in order of phase intensity (the primary phase listed first). The Haynes 188 and 230 are chromia-forming alloys. While chromia may have formed in the early stages of the Haynes 188 oxidation, these XRD results show that after 70h other complex oxides had formed. The Haynes 230 showed evidence of both  $\text{Cr}_2\text{O}_3$  and other complex oxides. The Haynes 214 is a possible chromia- or alumina-forming alloy. Neither of these oxides were observed by XRD. All three of these alloys formed significant amounts of spinel (oxides of the  $\text{AB}_2\text{O}_4$  structure) which are considered non-protective oxides. XRD of both the Kanthal A1 and PM2000 showed  $\alpha\text{-Al}_2\text{O}_3$  as the only oxide formed.

Table 2. Oxidation products of wires after exposure at 1204°C for 70h.

Alloy	Oxidation products	
	Dry Oxygen	50% H <sub>2</sub> O/50% O <sub>2</sub>
Haynes 188	NiWO <sub>4</sub> , NiCr <sub>2</sub> O <sub>4</sub> , NiO	NiO, NiCr <sub>2</sub> O <sub>4</sub>
Haynes 230	Cr <sub>2</sub> O <sub>3</sub> , NiCr <sub>2</sub> O <sub>4</sub> , NiO	--
Haynes 214	NiCr <sub>2</sub> O <sub>4</sub> /NiAl <sub>2</sub> O <sub>4</sub> , NiO	--
Kanthal A1	α Al <sub>2</sub> O <sub>3</sub>	α Al <sub>2</sub> O <sub>3</sub>
PM 2000	α Al <sub>2</sub> O <sub>3</sub>	(Fe,Cr) <sub>2</sub> O <sub>3</sub>

Typical morphologies of oxidized wire cross-sections are shown in Figure 4. It should be pointed out that the SEM/EDS results are obtained for those oxides that are retained on the oxidized wires. Some discrepancy with the XRD results may therefore be expected. The Haynes 188 shows complete consumption of the metal wire to form oxide phases. EDS analysis shows compositional layering of three oxide phases. In conjunction with the XRD results, these phases were identified as: 1) a Ni/Co rich oxide presumably (Ni,Co)O which is found on the surface of the wire and also in interior layers; 2) a Cr rich oxide corresponding to (Ni,Co)Cr<sub>2</sub>O<sub>4</sub>, and 3) the bright contrasting W-rich phase corresponding to (Co,Ni)WO<sub>4</sub>. EDS analysis in conjunction with XRD of the Haynes 230 wire cross-section indicated the oxide layer was predominantly Cr<sub>2</sub>O<sub>3</sub>. The Haynes 214 cross-section shows an inner layer of Al<sub>2</sub>O<sub>3</sub> formed at the metal interface. Outer layers of mixed spinels Ni(Cr,Al)<sub>2</sub>O<sub>4</sub> with NiO rich particles are also observed. Kanthal A1 wire cross-sections show α Al<sub>2</sub>O<sub>3</sub> oxide layers which are completely detached. The deformed shape of the oxide shells indicates the detachment probably occurred at temperature. EDS indicates aluminum is still present in the interior of the wire. PM2000 wire cross-sections also show α Al<sub>2</sub>O<sub>3</sub> oxide layers, however, these layers are adherent to the metal. A few areas of Cr<sub>2</sub>O<sub>3</sub> growth underneath the alumina are detected. Aluminum is depleted from the wire interior within the detection limit of EDS. Although the oxide is adherent, more interior voids are present in this wire than in the Kanthal A1. It has been suggested that oxide particles present in an alloy, such as Y<sub>2</sub>O<sub>3</sub> in PM2000, act as vacancy sinks and thereby eliminate void formation at the metal/oxide interface (15).

#### 50% H<sub>2</sub>O/50% O<sub>2</sub>

The weight change results for three alloy compositions after exposure in 50% H<sub>2</sub>O/50% O<sub>2</sub> at 1204°C for 70h are shown in Figure 5. The Haynes 188 wire showed initial large weight gains, again indicating failure to establish a protective scale or rapid breakaway oxidation. The weight gain reached a maximum at about 20 hours. This is similar to the time for complete metal consumption observed in dry oxygen. Instead of a weight plateau, a linear weight loss begins after complete oxidation. Also, the maximum weight gain is much less than observed in dry oxygen (about 7 mg/cm<sup>2</sup> in water vapor vs. 19 mg/cm<sup>2</sup> in dry oxygen). Deposits were found on the sapphire sample hanger downstream of the wire coil indicating volatilization and redeposition processes were occurring. These deposits were identified by XRD as WO<sub>3</sub> and NiWO<sub>4</sub>. Kanthal A1

showed parabolic kinetics similar to those observed in dry oxygen. Again spallation was observed on cooling. Finally, the PM2000 showed low oxidation kinetics until about 55 hours. A slight increase in weight gain rate was observed similar to the rate change observed in dry oxygen at 45 hours. In the last 2 hours of oxidation, the PM2000 showed rapid weight gain consistent with breakaway oxidation. This breakaway oxidation was not observed in dry oxygen and is in qualitative agreement with the more rapid transition to breakaway oxidation observed by Al-Badairy and Tatlock for cyclic oxidation of PM2000 coupons in moist air (13). This more rapid breakaway in moist air was attributed to enhancement of transient oxide formation in the earliest stages of oxidation causing slightly faster depletion of aluminum.

Macrographs of the wires after oxidation are shown in Figure 6. The Haynes 188 wire was again very brittle and damaged easily with handling. Evidence of spalling to bare metal was observed for the Kanthal A1 wire. No evidence of bare metal spalling was observed for the PM2000.

X-ray diffraction results for the oxidation products obtained in 50% H<sub>2</sub>O/50% O<sub>2</sub> are also included in Table 2. Oxidation products are again listed in order of phase intensity. The oxide formed on Haynes 188 was completely depleted in tungsten, and partially depleted in chromium relative to the oxides formed in dry oxygen. NiO was now the predominant oxide, followed by the spinel phase. The loss of tungsten from the oxide is consistent with the condensate collected downstream as discussed above. The oxide formed on the Kanthal A1 was  $\alpha$  Al<sub>2</sub>O<sub>3</sub>, unchanged from the product formed in dry oxygen. PM2000 oxidation products now contained (Fe,Cr)<sub>2</sub>O<sub>3</sub> rather than the slow growing  $\alpha$  Al<sub>2</sub>O<sub>3</sub>, consistent with the observed breakaway oxidation kinetics.

Typical morphologies of oxidized wire cross-sections are shown in Figure 7. The Haynes 188 again shows complete consumption of the metal wire to form oxides. EDS analysis shows compositional layering of three oxide phases plus layers of porosity. No tungsten is observed in these cross-sections, so the porosity presumably corresponds to loss of the NiWO<sub>4</sub> phase. In conjunction with the XRD results, the following three phases were identified: 1) a Ni/Co rich oxide presumably (Ni,Co)O which is found on the surface of the wire and also in interior layers; 2) a Cr rich oxide corresponding to (Ni,Co)Cr<sub>2</sub>O<sub>4</sub> spinel, and 3) a Ni,Co,Cr oxide phase with higher amounts of Ni and Co than the spinel phase. This third phase was not detected by XRD. Kanthal A1 wire cross-sections show  $\alpha$  Al<sub>2</sub>O<sub>3</sub> oxide layers which are completely detached. The deformed shape of the oxide layers indicates the detachment probably occurred at temperature. A significant number of the cross-sections are completely or partially missing the oxide shell, in contrast to the complete oxide shells observed in cross-sections of Kanthal A1 exposed in dry oxygen. It is uncertain whether this is due to more severe spalling conditions in water vapor, or handling of the wire after test. EDS indicates aluminum is still present in the interior of the wire. PM2000 wire cross-sections show various stages prior to and after initiation of breakaway oxidation. Adjacent wire cross-sections show a metallic wire with a primarily protective alumina scale next to a completely oxidized wire with remnants of an alumina scale overgrown by (Fe,Cr)<sub>2</sub>O<sub>3</sub>. Aluminum is completely depleted (within EDS detection limits) from the interior of those cross-

sections that are still metallic. The alumina layer is adherent for all cross-sections whether the interior is metallic or completely oxidized.

## DISCUSSION

### Relative alloy oxidation rates

The relative oxidation rates for the alloys were as expected. The Co-base Haynes 188 performed worse than the Ni-base Haynes 230. It is known that Co diffusion in CoO is more than 10 times faster than Ni diffusion in NiO (15). The slower growth rate of NiO allows a protective Cr<sub>2</sub>O<sub>3</sub> scale to become established on the Haynes 230. The Haynes 214 showed initially fast transient oxidation, then slowed to oxidation rates dominated by transport in the inner alumina layer. The slope of the weight gain curve after about 5 hours is similar to those for the alumina-forming Kanthal A1 and PM2000. In general, under the conditions examined here, the alumina forming alloys showed slower oxidation rates indicating more protective oxidation.

### Wire diameter effects

Wire diameter effects are of interest for several reasons. First, in this report, results for Kanthal A1 and PM2000 are compared. The Kanthal A1 wires were nominally 250  $\mu\text{m}$  in diameter, while the PM2000 wire was nominally 150  $\mu\text{m}$  in diameter. Since these are small diameter wires growing alumina scales, the reservoir of aluminum within the wire is important. The depletion rate is a function of both surface area and volume. For a given surface area, the 250 $\mu\text{m}$  wires have 1.7 times the volume of aluminum in reservoir relative to the 150 $\mu\text{m}$  wires. Thus, assuming parabolic kinetics until breakaway and shallow concentration profiles of aluminum in the alloy, breakaway oxidation, which occurred at 68h for the 150  $\mu\text{m}$  diameter wire in water vapor, would be expected to occur near 200h for a 250  $\mu\text{m}$  diameter wire all else being equal.

Second, the results in this paper for 150 to 250  $\mu\text{m}$  wires were obtained to examine oxidation behavior for potential alloys for hybrid seal applications. In hybrid seal applications, 40 to 125  $\mu\text{m}$  diameter wire is proposed for use to minimize gas leakage through the wire wrap or braid. These differences in surface to volume ratios are important for estimating lifetimes related to oxidation for different wire diameters. Clearly the oxidative lifetimes for wires in hybrid seal applications would be shorter than those for 150 to 250  $\mu\text{m}$  wires due to their smaller diameter.

Third, stresses in the growing oxide will vary with wire diameter. This will be discussed in further detail below.

### Effects of oxide volatility in water vapor

The weight change kinetics of the Haynes 188 in water vapor compared to those in dry oxygen are compared in Figure 8. Calculations of the stability of volatile hydroxides of the relevant oxides formed on the Haynes 188 alloy were made using FactSage Thermochemical Software (16) and are shown in Figure 9. This calculation was made using the SGTE pure substance database (17). Different results are obtained with the FACT database (16), although less hydroxide species are available in this database. Both data sets consistently predict that tungsten and nickel hydroxide species are very volatile. TGA of small diameter wires offers a powerful method for studying volatility of oxides formed in water vapor-containing environments. When oxide volatility occurs simultaneously with oxidation, it is difficult to deconvolute the weight loss due to volatility from the weight gain due to oxidation. Upon complete consumption of the alloy, however, the weight loss rate of the oxide becomes linear allowing a direct determination of oxide volatility. Monitoring the weight loss of completely oxidized alloy wires can be a useful technique to measure the relative stability of complex oxide phase assemblages actually formed on alloys in water vapor-containing environments.

### Stress induced spallation and geometry effects

The morphology of the detached oxide shells formed on the Kanthal A1 in dry oxygen indicates significant stresses were developed at temperature. Growth stresses in the oxide scale will vary with specimen geometry (8-12), increasing as the wire diameter decreases. The detached oxide shells formed on Kanthal A1 suggest the possibility of conducting experiments in which correlations between spallation and stress are determined as a function of wire diameter. Other factors which affect spallation, such as the reactive element additions in PM2000, clearly must be controlled to study wire diameter effects.

### Breakaway oxidation

The PM2000 results obtained in 50% H<sub>2</sub>O/50% O<sub>2</sub> indicate that TGA of a wire coil is an easy way to study breakaway kinetics. First, breakaway oxidation can be achieved in a short time due to the small diameter of the wire. Second, the exposure can be interrupted when the breakaway weight gain is at a predetermined value. Finally, a single cross-section through the coil offers a multitude of opportunities (e.g., about 30 different cross-sections of the wire) to observe the oxide morphology in various stages of breakaway as demonstrated in Figure 7c. Breakaway oxidation also been studied with thin foils and wedge-shaped coupons (18). Unlike wedge-shaped samples, use of small diameter wires does not require any pre-oxidation sample preparation. However, not all alloys are available in wire form.

## Recommendation for advanced hybrid seal wire selection

PM2000 is recommended as the prime candidate for advanced hybrid seal applications based on results of this study in which the wires were exposed to dry oxygen or 50% H<sub>2</sub>O/50% O<sub>2</sub> at 1204°C for 70h. The baseline Haynes 188 material showed rapid oxidation rates at this temperature. The chromia former Haynes 230 performed adequately in dry oxygen, however, chromia is known to be volatile in water vapor (19-21). Haynes 214 also performed adequately in dry oxygen, however, it has a lower aluminum content than the other alumina-forming alloys. Kanthal A1 and PM2000 oxidized slowly as expected for alumina formers, however, the scale formed on Kanthal A1 did not remain adherent. This would be a problem for seal applications where the wire overwrap is subjected to scrubbing against rough surfaces. While the PM2000 did undergo breakaway oxidation in water vapor and the Kanthal A1 did not, this is attributed to the differences in aluminum reservoir associated with the different wire diameters. Because hybrid seals are expected to experience temperature cycles in application, cyclic oxidation testing of the wires is now in progress. Final recommendations will be made at the conclusion of the cyclic testing.

## SUMMARY AND CONCLUSIONS

Small diameter wires (150 to 250 μm) of the high-temperature alloys Haynes 188, Haynes 230, Haynes 214, Kanthal A1 and PM2000 were oxidized at 1204°C in dry oxygen or 50% H<sub>2</sub>O/50% O<sub>2</sub> for 70 hours. PM2000 was recommended as the best candidate for hybrid seal applications based on the current test results. Thermogravimetric testing of small diameter wire coils offers useful capabilities for studying oxide scale volatility in water vapor, variations in growth stresses, and breakaway oxidation.

## ACKNOWLEDGMENTS

The authors would like to thank the following NASA GRC colleagues: Bruce Steinetz and Pat Dunlap for programmatic support, Jim Smialek for many helpful discussions, and Ralph Garlick for XRD. This work was funded by the NASA Next Generation Launch Technology Program.

## REFERENCES

- (1) J.J. DeMange, P.H. Dunlap, B.M. Steinetz, NASA/TM-2004-212898.
- (2) B.M. Steinetz, L.A. Kren, Z. Cai, "High Temperature Flow and Sliding Durability Assessments of Hypersonic Engine Seals," NASA TP-3483, December, 1994.
- (3) P. H. Dunlap, B.M. Steinetz, J.J. DeMange, NASA/TM-2004-212907.
- (4) B. Jonsson, A. Westerlund, G. Landor, pp. 324-335 in *European Federation of Corrosion Publications, 27 (Cyclic Oxidation of High Temperature Materials) 1999.*

- (5) T. Biegun, M. Danielewski, Z. Skrzypek, *Ox. Met.* 38 [3/4] 207-16, 1992.
- (6) F.W. Cole, J.B. Padden, A.R. Spencer, NASA/CR-1184 (1968).
- (7) S.K. Rhee, A.R. Spencer, *Met. Trans.* 1, 2021-2 (1970).
- (8) S. Mrowec, *Corrosion Science* 7, 563-78 (1967).
- (9) J. Romanski, *Corrosion Science* 8, 89-102 (1968).
- (10) P. Hancock, R.C. Hurst, pp. 1-84 in *Advances in Corrosion Science and Technology*, 4, eds. M.G. Fontana and R.W. Staehle, Plenum Press, NY (1974).
- (11) P. Kofstad, pp. 247-9 in *High Temperature Corrosion*, Elsevier Applied Science, NY (1988).
- (12) F. Nardou, L. Ranaivoniarivo, P. Raynaud, M. Billy, *Mat. Sci. & Eng.* 88, 241-6, 1987.
- (13) H. Al-Badairy, G.J. Tatlock, *Matl. At High. Temp.* 17 [1] 133-7, 2000.
- (14) H. Buscail, S. Heinze, Ph. Dufour, J.P. Larpin, *Ox. Met.* 47 [5/6] 445-464, 1997.
- (15) P. Kofstad, pp. 361-9, 404 in *High Temperature Corrosion*, Elsevier Applied Science, NY (1988).
- (16) C.W. Bale, P. Chartrand, S.A. Degterov, G. Eriksson, K. Hack, R. Ben Mahfoud, J. Melançon, A.D. Pelton, S. Petersen, *Calphad* 26 [2] 189-228 (2002).
- (17) I. Ansara, B. Sundman, pp. 154-158 in *Computer Handling and Dissemination of Data*, ed. P.S. Glaeser, Elsevier Science Publishers B.V., Amsterdam, The Netherlands, 1987.
- (18) H. Al-Badairy, G. Tatlock, pp. 1-14 in *High Temperature Corrosion and Materials Chemistry III*, ed. M. McNallan, E. Opila, Electrochemical Society, Inc., Pennington, NJ, 2001.
- (19) C.S. Tedmon, Jr., *J. Electrochem. Soc.* 113 [8] 766 (1966).
- (20) B.B. Ebbinghaus, *Combust. Flame*, 93, 119 (1993).
- (21) H. Asteman, J.-E. Svensson, L.-G. Johansson, M. Norell, *Ox. Met.* 52 [1/2] 95 (1999).

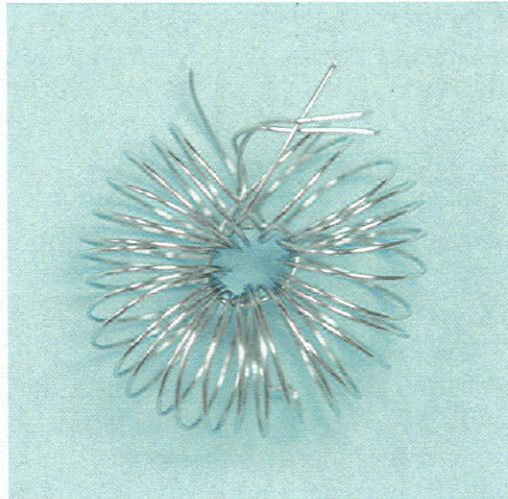


Figure 1. Typical macrograph of as-coiled wire before oxidation test.

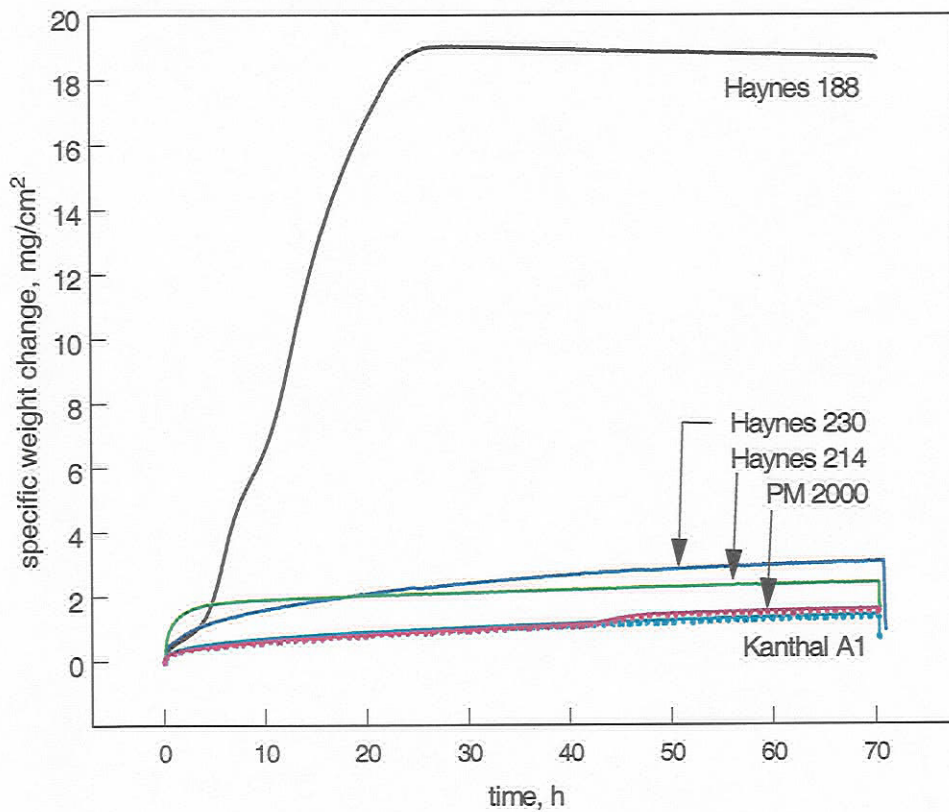


Figure 2. Specific weight change of wire samples oxidized at 1204°C in dry oxygen flowing at 0.4 cm/sec.

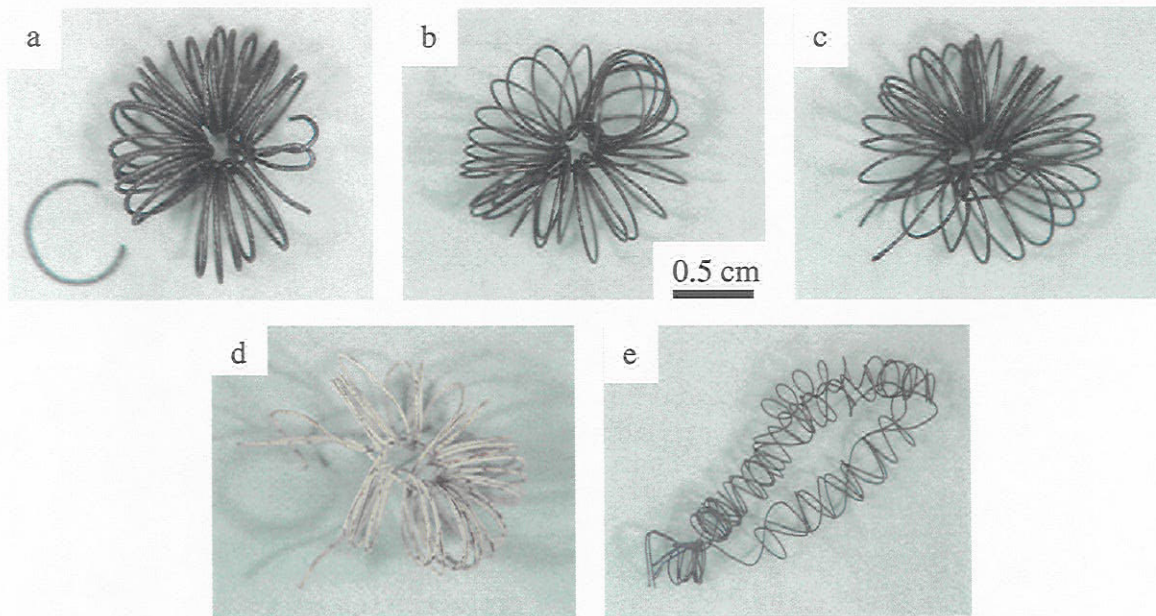


Figure 3. Macrographs of alloy wires after oxidation in dry oxygen at 1204°C for 70h:  
 a) Haynes 188, b) Haynes 230, c) Haynes 214, d) Kanthal A1, e) PM2000.

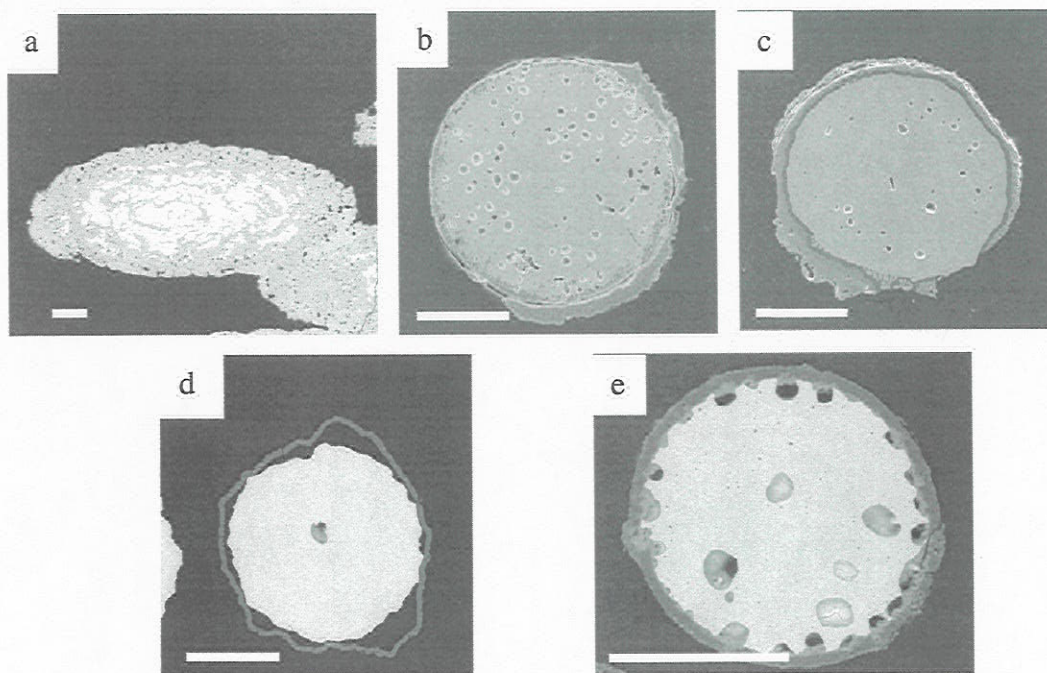


Figure 4. SEM cross-sections of wires after oxidation in dry oxygen at 1204°C for 70h:  
 a) Haynes 188, b) Haynes 230, c) Haynes 214, d) Kanthal A1, e) PM2000. The white bars in each micrograph represent 100 μm.

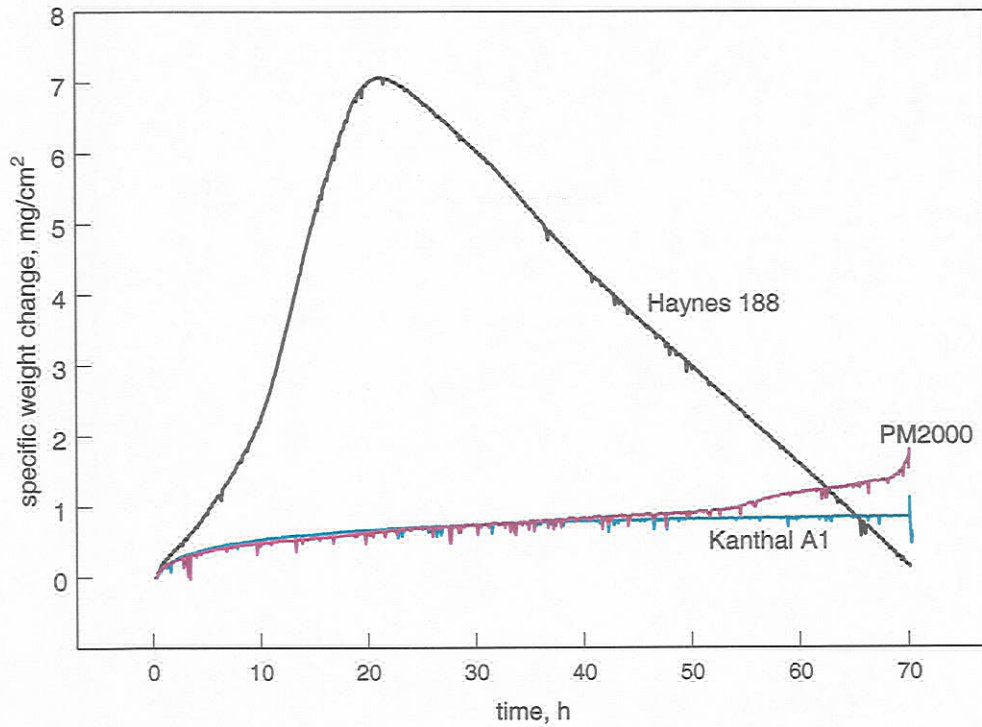


Figure 5. Specific weight change of wire samples oxidized at 1204°C in 50% H<sub>2</sub>O/50% O<sub>2</sub> flowing at 4.4 cm/s.

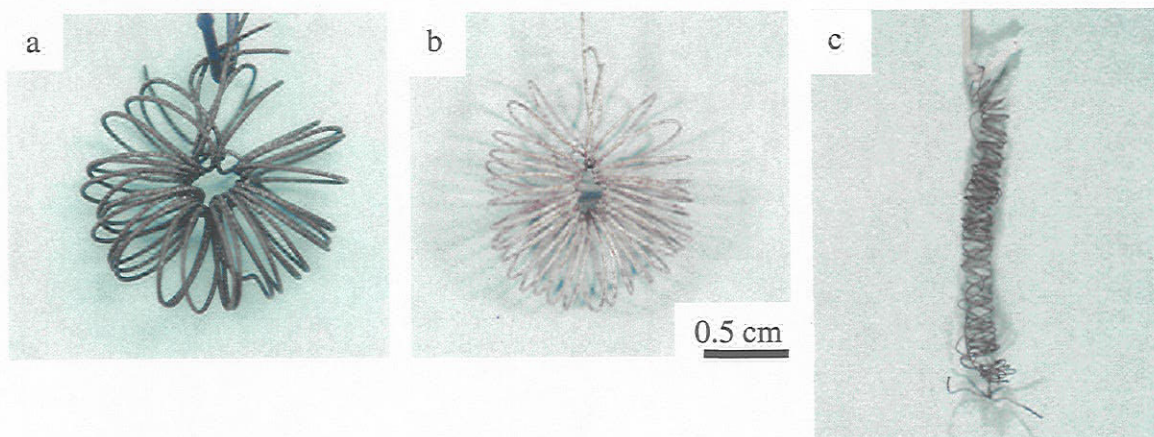


Figure 6. Macrographs of alloy wires after oxidation at 1204°C for 70h in 50% H<sub>2</sub>O/50% O<sub>2</sub> flowing at 4.4 cm/s: a) Haynes 188, b) Kanthal A1, c) PM2000.

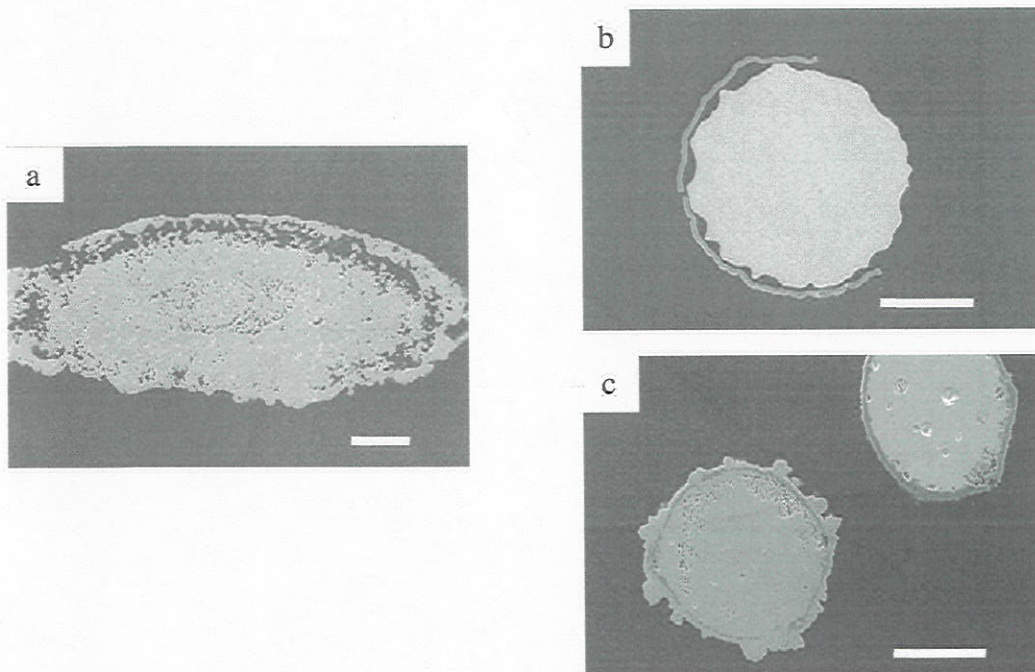


Figure 7. SEM cross-sections of wires after oxidation in at 1204°C for 70h in 50% H<sub>2</sub>O/50% O<sub>2</sub> flowing at 4.4 cm/s: a) Haynes 188, b) Kanthal A1, c) PM2000. The white bars in each micrograph represent 100 μm.

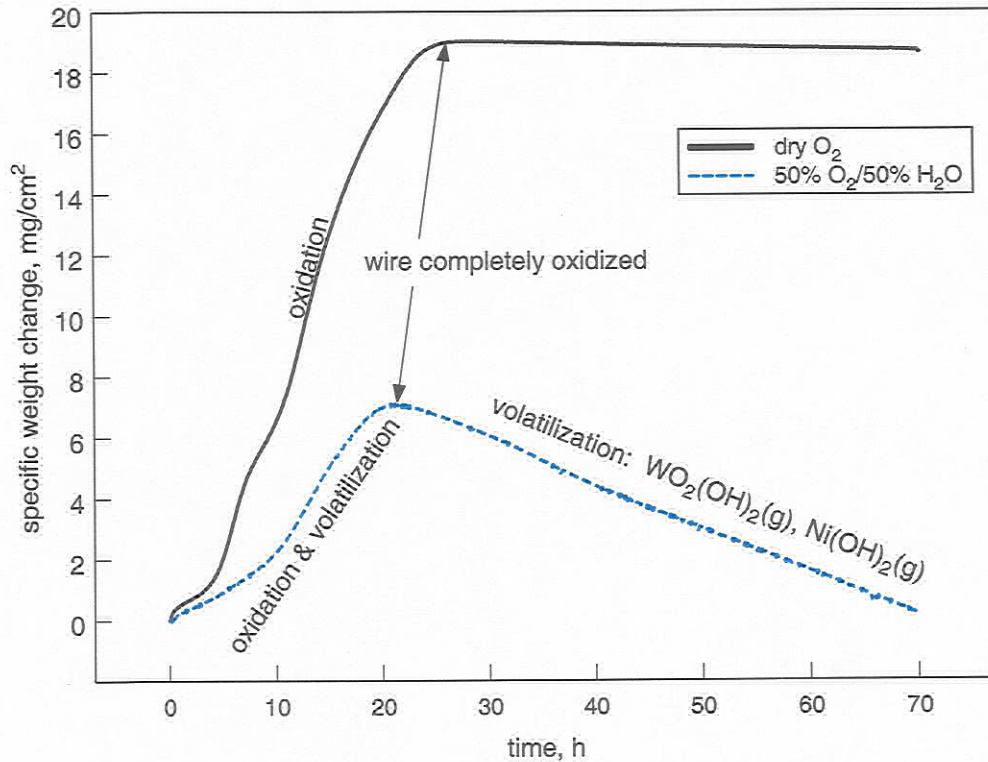


Figure 8. Specific weight change comparison for Haynes 188 wire oxidized in dry oxygen versus 50%H<sub>2</sub>O/O<sub>2</sub> at 1204°C.

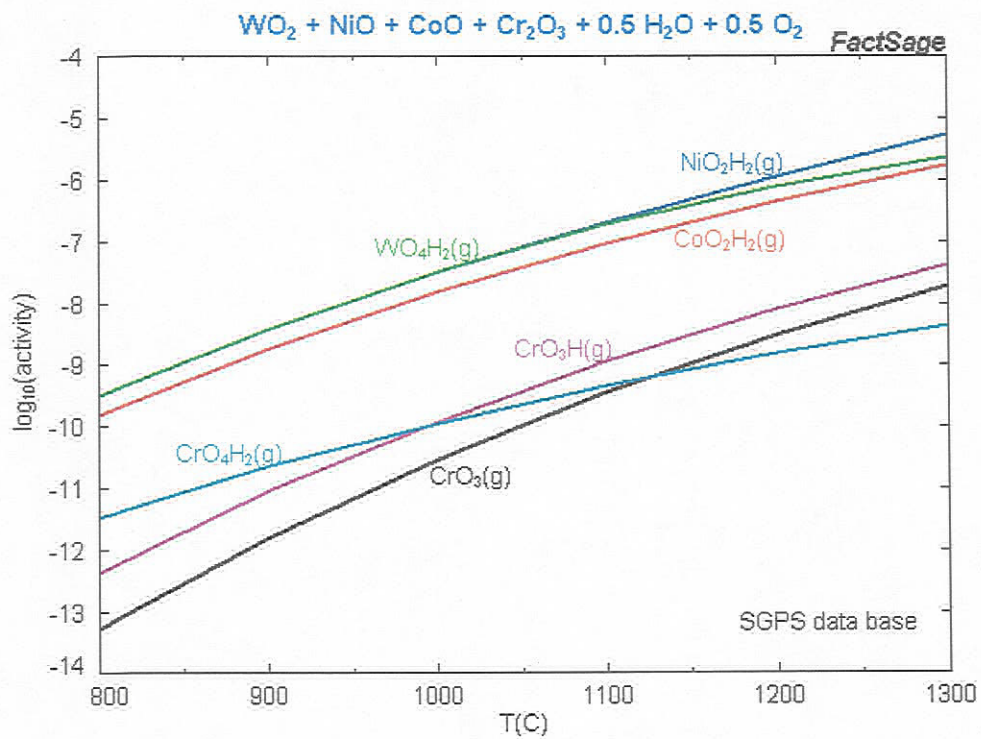


Figure 9. Calculated equilibrium partial pressures of volatile species for an assemblage of tungsten-, nickel-, cobalt-, and chrome-oxides in 50%  $\text{H}_2\text{O}$ /50%  $\text{O}_2$  at 1 atm.